

## Article

# Multi-Scenario Millimeter Wave Channel Measurements and Characteristic Analysis in Smart Warehouse at 28 GHz

Hang Mi <sup>1,2,3,4</sup> , Bo Ai <sup>1,2,3,4,5,6,\*</sup>, Ruisi He <sup>1,2,3,4,\*</sup>, Tong Wu <sup>7</sup>, Xin Zhou <sup>7</sup>, Zhangdui Zhong <sup>1,2,3,4</sup>, Haoxiang Zhang <sup>8</sup> and Ruifeng Chen <sup>9</sup>

- <sup>1</sup> State Key Laboratory of Advanced Rail Autonomous Operation, Beijing Jiaotong University, Beijing 100044, China; hangmi@bjtu.edu.cn (H.M.); zhdzhong@bjtu.edu.cn (Z.Z.)
  - <sup>2</sup> Frontiers Science Center for Smart High-Speed Railway System, Beijing Jiaotong University, Beijing 100044, China
  - <sup>3</sup> Key Laboratory of Railway Industry of Broadband Mobile Information Communications, Beijing Jiaotong University, Beijing 100044, China
  - <sup>4</sup> Beijing Engineering Research Center of High-Speed Railway Broadband Mobile Communications, Beijing Jiaotong University, Beijing 100044, China
  - <sup>5</sup> Henan Joint International Research Laboratory of Intelligent Networking and Data Analysis, Zhengzhou University, Zhengzhou 450001, China
  - <sup>6</sup> PengCheng Laboratory, Shenzhen 518000, China
  - <sup>7</sup> National Institute of Metrology of China, Beijing 100029, China; wut@nim.ac.cn (T.W.); zhouxin@nim.ac.cn (X.Z.)
  - <sup>8</sup> China Academy of Industrial Internet, Ministry of Industry and Information Technology, Beijing 100102, China; zhx61778294@126.com
  - <sup>9</sup> Institute of Computing Technology, China Academy of Railway Sciences, Beijing 100081, China; ruifeng\_chen@126.com
- \* Correspondence: boai@bjtu.edu.cn (B.A.); ruisi.he@bjtu.edu.cn (R.H.)

**Abstract:** Smart warehouses are revolutionizing traditional logistics operations by incorporating advanced technologies such as Internet of Things, robotics, and artificial intelligence. In these complex and dynamic environments, control and operation instructions need to be transmitted through wireless networks. Therefore, wireless communication plays a crucial role in enabling efficient and reliable operations. Meanwhile, channel measurements and modeling in smart warehouse scenarios are essential for understanding and optimizing wireless communication performance. By accurately characterizing radio channels, communication systems can be better designed and deployed to meet unique challenges in smart warehouse scenarios. In this paper, we present an overview of smart warehouse scenarios and explore channel characteristics in smart warehouse scenarios. We conducted a measurement campaign for millimeter wave radio channels in smart warehouse scenarios. A vector network analyzer-based channel sounder was exploited to record channel characteristics at 28 GHz. Based on the measurements, large-scale channel parameters, including path loss, root-mean-square (RMS) delay spread, and Rician  $K$  factor were investigated. The unique channel characteristics in smart warehouse scenarios were explored.

**Keywords:** channel measurement; channel characteristics; mmWave channel; smart warehouse



**Citation:** Mi, H.; Ai, B.; He, R.; Wu, T.; Zhou, X.; Zhong, Z.; Zhang, H.; Chen, R. Multi-Scenario Millimeter Wave Channel Measurements and Characteristic Analysis in Smart Warehouse at 28 GHz. *Electronics* **2023**, *12*, 3373. <https://doi.org/10.3390/electronics12153373>

Academic Editor: Martin Reisslein

Received: 10 July 2023

Revised: 3 August 2023

Accepted: 4 August 2023

Published: 7 August 2023



**Copyright:** © 2023 by the authors. Licensee MDPI, Basel, Switzerland. This article is an open access article distributed under the terms and conditions of the Creative Commons Attribution (CC BY) license (<https://creativecommons.org/licenses/by/4.0/>).

## 1. Introduction

Smart warehouses have emerged as a transformative force in the logistics industry, leveraging cutting-edge technologies to optimize operations and enhance efficiency. By integrating Internet of Things (IoT) devices, autonomous robots and artificial intelligence (AI), these intelligent warehousing environments offer unprecedented levels of automation and real-time data-driven decision-making [1,2]. These intelligent warehousing environments incorporate a multitude of interconnected devices, such as sensors, RFID tags, and autonomous robots, creating a vast network of IoT-enabled entities [3,4]. With the

integration of AI and machine learning algorithms, smart warehouses can efficiently monitor and manage inventory, streamline order fulfillment, and automate material handling tasks [5]. Therefore, smart warehouses have revolutionized traditional logistics operations, paving the way for enhanced efficiency, improved inventory management, and accelerated order fulfillment.

The integration of autonomous robots and AI-powered systems has transformed material handling processes within smart warehouses [6]. Robots equipped with sensors and navigation capabilities can autonomously navigate the warehouse floor, retrieve and transport items, and even collaborate with human workers. This combination of human–robot collaboration improves operational efficiency and ensures worker safety by offloading repetitive and physically demanding tasks to machines [7,8]. Furthermore, AI algorithms continuously learn from data generated within the warehouse, enabling predictive maintenance of equipment, intelligent route planning, and optimization of storage space.

In recent years, the 5th generation mobile communication (5G) has been offering higher data rates and wider connectivity. Meanwhile, applications in vertical industries are also important in 5G networks, such as transportation [9] and industrial IoT [10]. The 5G network will serve as the lifeline of these interconnected systems in smart warehouses. It enables seamless and real-time communication between the various components of the ecosystem in smart warehouses, such as robots, sensors, inventory management systems, and workers [11]. Through wireless connectivity, critical information is transmitted and received, enabling effective coordination, monitoring, and control of warehouse operations. For example, real-time inventory updates can be communicated to the central management system, ensuring accurate stock levels and facilitating efficient order fulfillment [12]. Wireless networks also enable workers to receive instructions, collaborate with robots, and access relevant data and instructions through wearable devices or handheld terminals [13]. Therefore, smart warehouses heavily rely on wireless networks for efficient and seamless operations.

Millimeter wave (mmWave) communication plays a crucial role in 5G networks. For example, mmWave communication can deliver ultra-fast data rates, high network capacity, and low-latency connectivity [14–17]. Due to the wider available bandwidth, mmWave systems enable multi-gigabit per second transmission speeds, unlocking the potential for bandwidth-intensive applications and services such as high-definition video streaming, virtual reality experiences, and real-time IoT applications [18–21]. Moreover, the low latency offered by mmWave communication enables near-instantaneous response times. That is critical for time-sensitive applications such as autonomous vehicles, remote surgery, and industrial automation. Therefore, the advantages of mmWave communication will further promote the development of smart warehouses. For example, mmWave technology enables real-time and high-bandwidth communication for seamless coordination between autonomous robots, workers, and management systems in smart warehouses. This facilitates efficient material handling, inventory management, and order fulfillment processes. Due to shorter wavelengths and beamforming applications, mmWave communication supports more precise asset tracking and localization within the warehouse environment, enabling accurate monitoring of inventory, equipment, and personnel [22,23]. This enhances inventory accuracy and ensures worker safety. In addition, mmWave communication enables high-resolution video transmission, providing real-time monitoring of critical areas, theft prevention, and incident response. These applications of mmWave communication contribute to the optimization of operations, increased productivity, and improved overall performance in smart warehouses.

Channel modeling is one of the most basic research areas in wireless communications, and the performance of communication systems depends on channel characteristics [24–26]. However, few studies have focused on mmWave channel measurements in smart warehouses. Ref. [27] conducted mmWave channel measurements in a smart warehouse scenario but it only shows power delay profile and path loss results. Other channel characteristic parameters were not analyzed. It should be noted that industrial scenarios have some

similarities with smart warehouse scenarios. For example, automated robots are heavily deployed in both scenarios. Meanwhile, robots and other automated equipment are mostly made of metal, which can generate stronger reflection paths compared with conventional indoor scenarios. The similarity of the two scenarios can compensate for the absence of channel measurements in smart warehouses to a certain extent. Due to the implementation of concepts such as industry 4.0 and the industrial Internet of Things, channel measurement and modeling in industrial scenarios are also gradually emerging. For example, Ref. [28] conducted mmWave channel measurement in industrial scenarios at 60 GHz, and modeled channel characteristic parameters. Channel measurement results for two different industrial scenarios are provided in [29]. Measurement results show that metallic surfaces in industrial scenarios generate a large number of reflection paths. Furthermore, channel measurements and modeling for other mmWave frequency bands in industrial scenarios were also conducted, such as 28 GHz [30–32]. Among them, 3.7 GHz and 28 GHz channel measurements were conducted in [32], and the channel characteristic difference between sub-6 GHz and mmWave was extracted and compared. However, channel measurement in smart warehouses still cannot be replaced by industrial scenarios. For example, the dynamic characteristics of channels in smart warehouses will be more pronounced. The movement of goods will change the layout of a warehouse, thereby affecting radio channels. Meanwhile, the operation of robots also significantly improves dynamic characteristics. Line-of-sight (LOS) paths between transceivers will be blocked by moving objects. This is significantly different from the industry scenario. Therefore, mmWave channel measurements campaigns in smart warehouses are still necessary for channel characteristic analysis and modeling.

In this paper, we conducted mmWave channel measurements in smart warehouse scenarios at 28 GHz. The smart warehouse scenarios include three different sub-scenarios, which are an intelligent forklift truck scenario, a stacking and shuttle car scenario, and an automated guided vehicles (AGVs) scenario. The three sub-scenarios have different environment layouts and operation methods, and use different robots and autonomous vehicles. This leads to significant differences in radio channels. The large-scale channel parameters were characterized based on the conducted channel measurements in smart warehouse scenarios. The large-scale channel parameters, including path loss, root-mean-square (RMS) delay spread, and Rician  $K$  factor, were calculated. The statistical properties of large-scale channel parameters were extracted and analyzed in different sub-scenarios. Among them, the fitted model parameters can be used as a reference to be generalized to other smart warehouse environments or similar scenarios. The work in this paper will help researchers understand radio channels for designing communication systems in smart warehouse scenarios.

The rest of this paper is organised as follows. Section 2 elaborates the measurement scenarios and specifications in the measurement campaign. Section 3 presents the extraction and analysis results of key large-scale channel parameters. Finally, conclusive remarks are included in Section 4.

## 2. MmWave Channel Measurement Campaigns in Smart Warehouse

In this paper, we conducted channel measurement in the smart warehouse scenario at a 28 GHz frequency band. A vector network analyzer (VNA)-based channel sounder was used in the measurement. The transmitter (Tx) uses a horn antenna. The frequency range of the Tx antenna is 26.5–40 GHz. The center frequency of the channel measurement is 28 GHz, and the bandwidth is 1 GHz. The gain of the Tx antenna is 20.3 dBi and is almost constant over the frequency range of the channel measurement. The half-power beamwidth (HPBW) of the Tx antenna is  $21^\circ$ . The receiver (Rx) was equipped with a uniform planar array (UPA) antenna, which contains  $4 \times 8 = 32$  microstrip elements that are vertically polarized. Each array element is measured and calibrated in an anechoic chamber to obtain a 3D antenna pattern. The radio frequency (RF) in Rx is traversed and connected to each antenna element through electronic switching. Based on the calibration results of the Rx antenna

array, the Space-Alternating Generalized Expectation-Maximization (SAGE) algorithm [33] is used to estimate and extract MPCs information. Figure 1 shows the structure diagram of mmWave channel sounder system. Among them, the mmWave RF signal transceiver includes up and down converter modules. A power amplifier was equipped with RF signal transmitters. Meanwhile, the RF signal receiver was equipped with a low-noise amplifier. The parameters related to the measurement configuration are summarized in Table 1, and the detailed structure of the channel sounder is presented in [34].

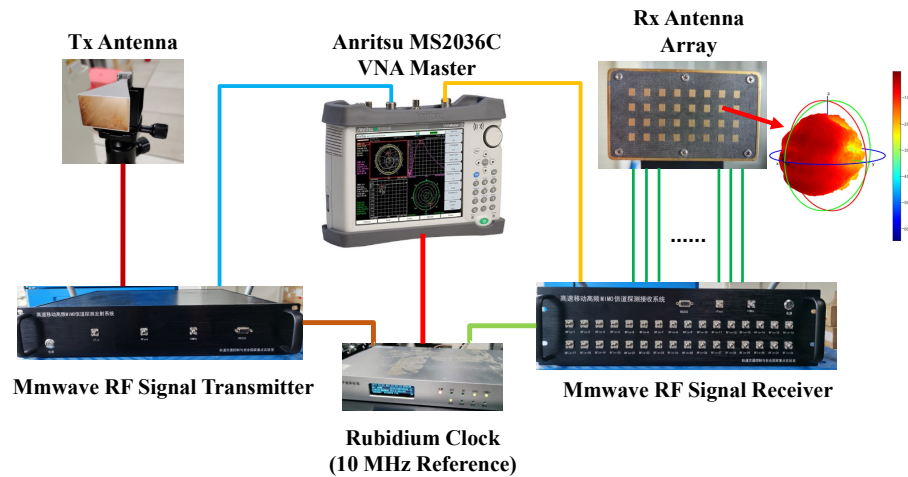


Figure 1. Structure diagram of mmWave channel sounder system.

Table 1. Configurations of measurement system.

Parameter	Value
Frequency	28 GHz
Bandwidth	1 GHz
Number of frequency point	1001
Delay resolution	1 ns
Intermediate frequency bandwidth	500 Hz
Tx antenna	Horn antenna
Rx antenna	4 × 8 array antenna
Transmit power	20 dBm
Maximum excess delay	1000 ns
Maximum MPCs length	300 m

A smart warehouse is equipped with various robots and AGVs. They perform corresponding tasks or transport different types of goods. In this paper, we conducted channel measurements for three sub-scenarios in a smart warehouse—an intelligent forklift truck, a stacking shuttle car, and AGVs. In the measurement campaign, the position of Tx was fixed, and Rx moved away from Tx gradually. The boresight of the Tx and Rx antennas were always steering towards each other.

### 2.1. Intelligent Forklift Truck Scenario

In a smart warehouses, intelligent forklift trucks are mainly used for the handling of bulky goods. Equipped with advanced navigation systems, sensors, and automation capabilities, intelligent forklift trucks streamline and optimize various tasks. They autonomously navigate through the warehouse, efficiently picking up and transporting goods to their designated locations. By integrating with inventory tracking systems, they ensure accurate inventory management in real-time, minimizing errors and manual effort. In addition, intelligent forklift trucks contribute to optimal space utilization by identifying vacant slots and maximizing storage density. They enhance safety with collision detection sensors, mitigating the risk of accidents. The work of the intelligent forklift truck is divided into unloading and loading. During the process of unloading and warehousing, the intelligent

forklift accesses the connection with the central control system through a wireless network. The truck parking channel is determined through wireless instructions and the goods are taken out and put into the roadway allocated by the central control system. In the process of loading and leaving the warehouse, the intelligent forklift truck receives instructions from the central control system through the wireless network. Then, the goods for the same destination are sent to the same area to be collected and put into the truck compartment.

For channel measurement in the intelligent forklift trucks scenario, Figure 2 illustrates a top-view geometry of its environment and measurement positions. Figure 3 shows photos of the intelligent forklift trucks scenario. It can be observed that the shelf and intelligent forklifts make up the objects in this scenario. The Tx was at one end of the shelf. The Rx gradually moves from the other end towards the Tx, as shown in Figure 2. Among them, the distance between each Rx position is 1 m. The shortest distance between Tx and Rx is 5 m.

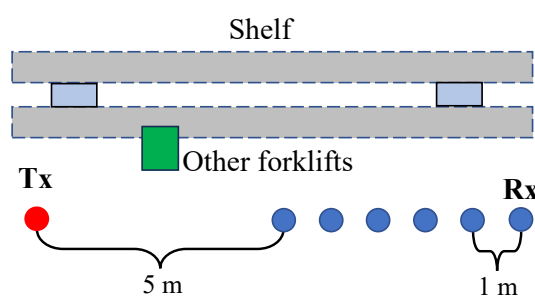


**Figure 2.** Top-view sketch of channel measurement in intelligent forklift trucks scenario.

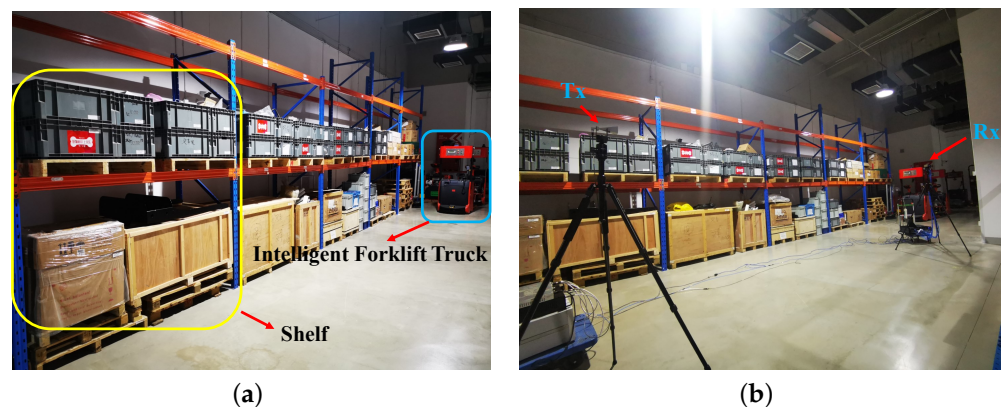


**Figure 3.** Photos of intelligent forklift trucks scenario. (a) Racking and intelligent forklift truck. (b) Tx and Rx measurement positions.

## 2.2. Stacking and Shuttle Car Scenario

The shuttle cars for stacking are responsible for vertical storage. Equipped with lifting mechanisms, they can retrieve pallets or goods from high racks and place them in their designated locations with precision, as shown in Figure 4. Figure 4a,b illustrate the process of unloading and loading. The red arrow in Figure 4 indicates the moving direction of the goods. Stacking cars optimize space utilization by efficiently stacking pallets and maximizing vertical storage capacity. They work in conjunction with warehouse management systems to retrieve items based on real-time inventory data, ensuring accurate and timely order fulfillment.

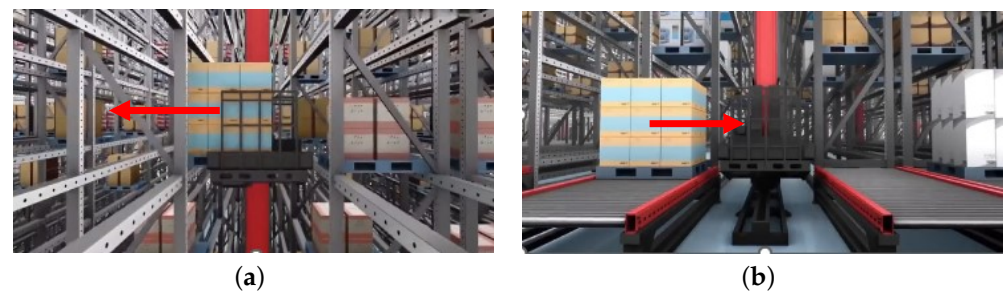


**Figure 4.** Working process of stacking and shuttle car. (a) Unloading. (b) Loading.

In the process of loading and unloading the three-dimensional warehouse, the stacking and the shuttle car receive instructions from the central control system through the wireless network. In this way, the specific position of goods in the warehouse can be determined and the precise insertion and removal of goods can be realized. However, there are metal steel frames throughout the stacking. These steel frames can block MPCs or generate powerful reflected MPCs, which enhances the variation of the channel. We conducted channel measurements in the stacking and shuttle car scenario. The top-view geometry of the environment and measurement positions are illustrated in Figure 5a. Among them, the gray part represents stacking. The Tx is located outside the stack, and the Rx is located inside the stack. Figure 5b shows a photograph of the measurement campaign and relative positions of the transceiver. Similar to the measurement campaign in the intelligent forklift truck scenario, the distance between each Rx position is 1 m, and the shortest distance between Tx and Rx is 5 m.

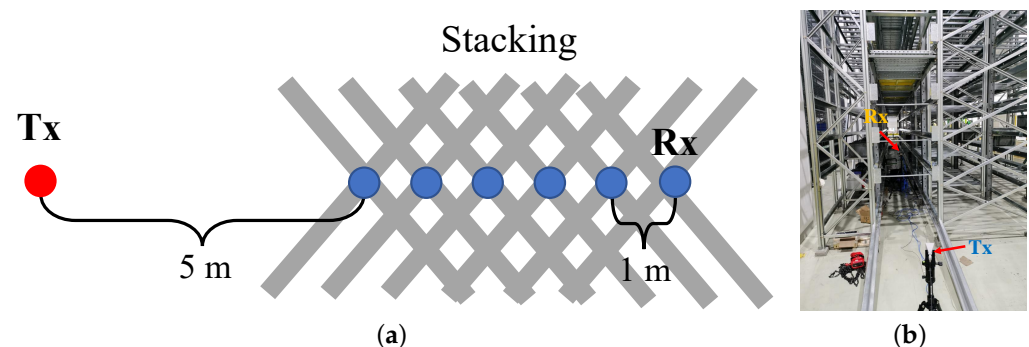


**Figure 5.** Channel measurement in stacking and shuttle car scenario. (a) Top-view sketch. (b) Photo of measurement campaign.

### 2.3. Automated Guided Vehicle Scenario

The AGVs play an important role in smart warehouses by revolutionizing material handling and logistics operations. AGVs are autonomous vehicles equipped with sensors, cameras, and navigation systems, enabling them to navigate and transport goods within the warehouse environment without human intervention. They follow predefined traces or dynamically adjust their routes through real-time communication, optimizing travel traces and reducing congestion. AGVs can perform a variety of tasks, including picking up and delivering items, moving pallets, and replenishing inventory. They seamlessly integrate with warehouse management systems and other automation technologies, allowing for efficient coordination and synchronization of operations. AGVs enhance productivity by reducing manual labor, streamlining workflows, and minimizing errors in goods transportation. The deployment of AGVs in smart warehouses improves efficiency, accuracy, and safety.

Figure 6 shows typical AGVs in a smart warehouse. The AGV receives instructions from the central control system through the wireless network. According to the optimal

route planned, the goods are sent to the storage position in a waiting area. After receiving product order information, the AGV will accurately find the product and send it to the picking workstation according to the optimal trace.



**Figure 6.** Typical AGVs in a smart warehouse.

Figure 7 illustrates the measurement campaign in the AGVs scenario. Figure 7a shows the top-view sketch. The interval between Rx positions is 1 m. The shortest distance between Tx and Rx is 5 m. There are freight containers randomly distributed around the transceiver, as shown in the green box in Figure 7a. It should be noted that different AGVs have different routes in actual work. Therefore, the LOS path between transceivers can be blocked by other AGVs. Considering the occurrence of blocking, we conducted channel measurements under LOS and obstructed line-of sight (OLOS) conditions, respectively. Among them, the LOS path is blocked by the freight container under OLOS conditions, as shown in the gray box in Figure 7a. Figure 7b illustrates a photo of the measurement campaign in the AGVs scenario.

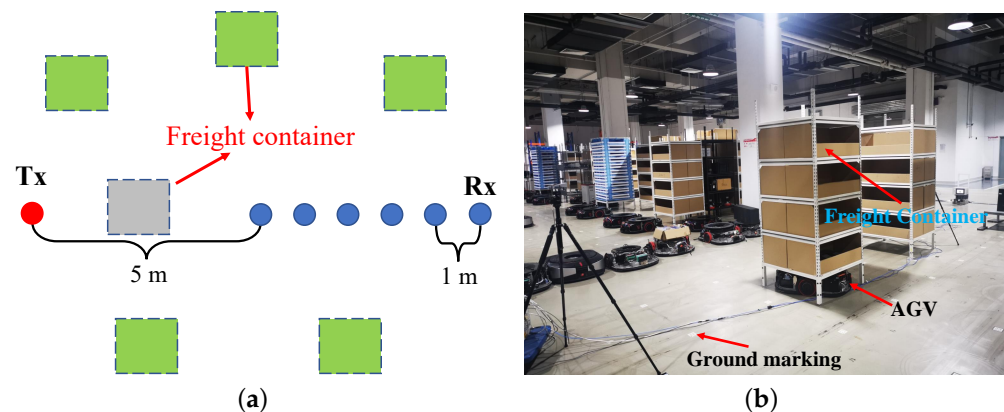


**Figure 7.** Channel measurement in AGVs scenario. (a) Top-view sketch. (b) Photo of measurement campaign.

### 3. Channel Characteristics

The 3rd Generation Partnership Project (3GPP) contains a diversity of deployment scenarios such as Urban Micro (UMi), Urban Macro (UMa), indoor office, indoor shopping mall, etc. However, in the existing literature and standard organizations, there are few parameter extraction results from a channel model in smart warehouse scenarios. In this section, the key large-scale channel parameters are analyzed based on the channel measurements described in Section 2. The fitting parameters of the channel model are extracted to fill the gap in smart warehouse scenarios. The key large-scale channel parameters include path loss, RMS delay spread, and Rician  $K$  factor.

#### 3.1. Path Loss

Path loss is commonly used to evaluate propagation loss between transceivers. Meanwhile, it is one of the most intuitive parameters with which to describe channel characteris-

tics. The path loss can be determined by channel transfer function  $H(f_l)$  as follows [35]:

$$PL = -10 \log_{10} \left( \frac{1}{N_f} \sum_{l=1}^{N_f} |H(f_l)|^2 \right), \quad (1)$$

where  $N_f$  is the number of measured frequency points. In addition, the floating-intercept model (also known as AB model) is explored in order to better characterize the variation of path loss. It offers a standard model and is adopted by 3GPP [36] and WINNER II [37]. Meanwhile, the AB model has been extended and validated in the mmWave frequency band [38,39]. It is defined as [38]:

$$PL[\text{dB}] = 10\alpha \log_{10}(d) + \beta + X_{\sigma_{\text{sf}}}, \quad (2)$$

where  $d$  is the distance between transceivers,  $\alpha$  is coefficient showing the dependence of path loss on distance, and  $\beta$  is an optimized offset value for path loss in decibels. Their values are related to the propagation environment and deployment of the transceivers.  $X_{\sigma_{\text{sf}}}$  is the shadow fading, which is a zero-mean Gaussian distribution, with a standard deviation of  $\sigma_{\text{sf}}$ . In addition, free-space path loss is also introduced for comparison with the measured loss, which is defined as [40]:

$$FSPL[\text{dB}] = 20 \log_{10} \frac{4\pi d}{\lambda}, \quad (3)$$

where  $\lambda = c/f$  is the wavelength,  $c$  is the speed of light, and  $f$  is the carrier frequency. The fitted parameters of the AB model are summarized in Table 2. Figures 8 and 9 illustrate the path loss and fitting results using the AB model for three smart warehouse scenarios. In Figure 8a, the measured path loss is slightly smaller than the free-space path loss in the intelligent forklift truck scenario. This is because the metal shelf around the transceiver generates reflection MPCs, which increases the received power. For the stacking and shuttle car scenario, it is found from Figure 8b that the measured and fitted path loss is significantly larger than those of the free-space path loss and the intelligent forklift truck scenario. This is mainly due to the fact that the Rx is located in the stack, and the LOS path can be obstructed by metal brackets in the stack. For the path loss of the AGV scenario in Figure 9, it is found that the measured and fitted path loss is close to the free-space path loss under the LOS condition. This demonstrates that the MPCs generated by other freight containers do not contribute significantly to the improvement of received power. The path loss under the OLOS condition is significantly lower than that under the LOS condition and free-space path loss. This means that the obstruction of freight containers can significantly attenuate the received power for Rx. Therefore, more careful route planning is required in smart warehouses to avoid OLOS conditions by obstructions. In addition, it is found from Table 2 that the stacking and shuttle car scenario shows larger  $\alpha$  and smaller  $\beta$  ( $\alpha = 3.94$ ,  $\beta = 50.41$  dB) in the AB model compared to the other scenarios. Meanwhile,  $\alpha$  and  $\beta$  in the other existing indoor LOS scenarios are also significantly different from the stacking and shuttle car scenario, such as the library scenario ( $\alpha = 1.80$ ,  $\beta = 65.82$  dB) [41] and the hall scenario ( $\alpha = 0.96$ ,  $\beta = 76.72$  dB) [39]. Larger  $\alpha$  and smaller  $\beta$  indicate a rapid increase in path loss as the distance between transceivers increases, which is also shown in Figure 8b. Therefore, the impact of stacking on path loss becomes more pronounced with increasing distance. In addition, in the OLOS condition of the AGVs scenario,  $\alpha$  and  $\beta$  are similar to the LOS condition of the AGVs scenario and the intelligent forklift truck scenario, and are also close to the library scenario [41]. This indicates that the freight containers cause additional transmission loss, but does not make the path loss increase rapidly with distance.

**Table 2.** Fitted AB model parameters of path loss.

Scenarios	Parameters		
	$\alpha$	$\beta$	$\sigma_{sf}$
Intelligent forklift truck	1.82	61.75	0.32
Stacking and shuttle car	3.94	50.41	3.47
AGV (LOS)	1.63	64.23	0.31
AGV (OLOS)	1.93	66.15	0.86

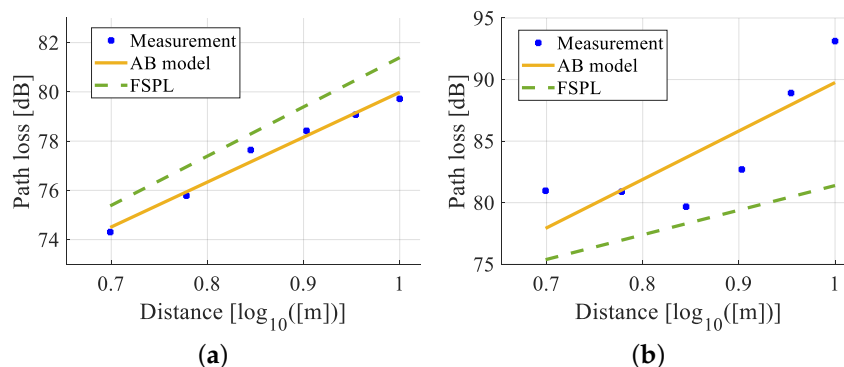


**Figure 8.** (a) Path loss for intelligent forklift truck scenario. (b) Path loss for stacking and shuttle car scenario.

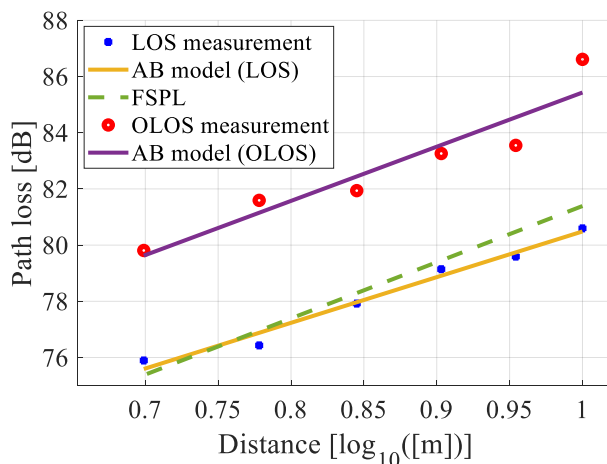


**Figure 9.** Path loss for AGVs scenario.

3.2. RMS Delay Spread

RMS delay spread is a crucial parameter that characterizes the time dispersion of the radio channel. It measures the spread of different propagation paths in terms of delay, providing insights into the channel to support reliable communication. The RMS delay spread can be calculated as the second-order central moment of the power delay profile, and it is expressed as [42]:

$$\tau_{rms} = \sqrt{\frac{\sum_{i=1}^N P_i(\tau_i)^2}{\sum_{i=1}^N P_i} - \left(\frac{\sum_{i=1}^N P_i\tau_i}{\sum_{i=1}^N P_i}\right)^2}, \tag{4}$$

where  $\tau_i$  represents the delay and  $P_i$  describes the power of the corresponding delay. Figure 10 illustrates the empirical cumulative distribution functions (CDFs) of RMS delay spread represented in logarithm scales for all smart warehouse scenarios. Typically, the log-normal distribution is used to characterize the RMS delay spread [43]. Therefore, the

empirical CDFs are well fitted with normal distributions. The parameters of fitted CDFs for RMS delay spread are summarized in Table 3. It can be observed from Figure 10 that the RMS delay spread in the shuttle car scenario is significantly smaller than in the other two scenarios. The steel frames in the stack can generate strong reflection paths. However, the strong reflection paths can be obstructed by steel frames as well due to the dense distribution. In the intelligent forklift truck and AGV scenarios, the reflection paths generated by shelf and freight containers increase the richness of MPCs and lead to larger RMS delay spread.

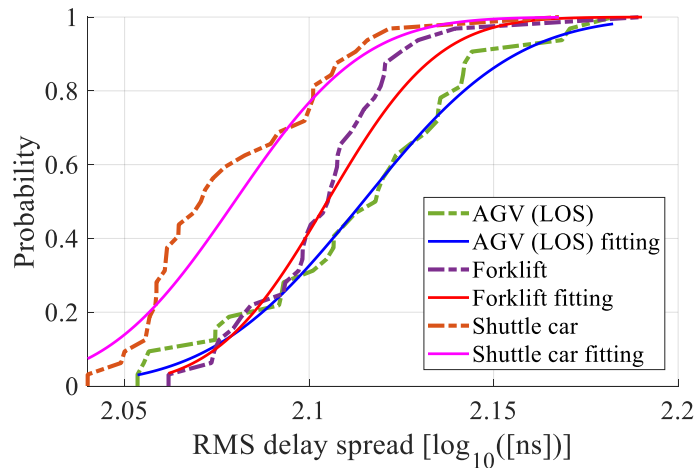


Figure 10. Empirical and fitted CDFs of RMS delay spread.

Table 3. Parameters of fitted CDFs for RMS delay spread.

Scenarios	Parameters	
	$\mu_{\log\text{-normal}}$	$\sigma_{\log\text{-normal}}$
Intelligent forklift truck	2.10	0.024
Stacking and shuttle car	2.08	0.028
AGV (LOS)	2.11	0.033

### 3.3. Rician K Factor

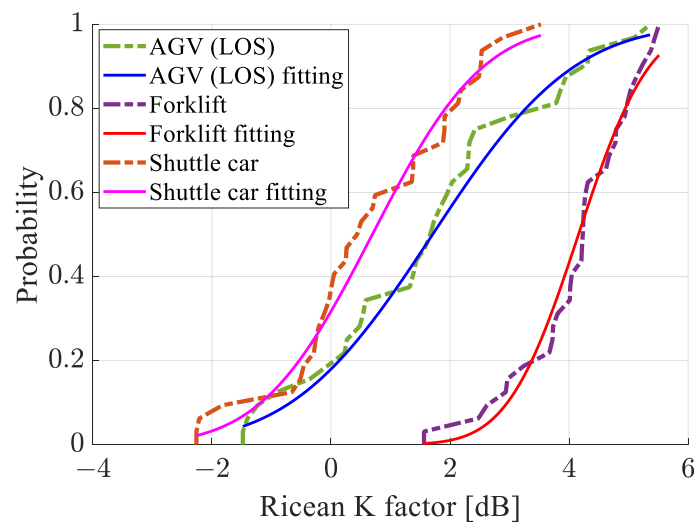
The Rician  $K$  factor is defined as the ratio of signal power of LOS path to that of other MPCs. It is expressed as [44]:

$$KF = 10 \log_{10} \left( \frac{P_{LOS}}{\sum_{i=1}^N P_i - P_{LOS}} \right), \tag{5}$$

where  $P_{LOS}$  is the power of LOS path and  $P_i$  denotes the power of  $i$ -th MPC. It is found from Equation (5) that the Rician  $K$  factor describes the power contribution of the LOS path to the sum of all MPCs. Similar to RMS delay spread, the log-normal distribution is used to characterize the Rician  $K$  factor as well. Figure 11 illustrates the empirical cumulative distribution functions (CDFs) of Rician  $K$  factor represented in logarithm scales for all smart warehouse scenarios, and the parameters of fitted CDFs for Rician  $K$  factor are listed in Table 4. It is found that the Rician  $K$  factor of the intelligent forklift truck scenario is significantly larger than that of the other scenarios. This is mainly due to the fact that the intelligent forklift truck scenario is relatively empty compared to the other scenarios; only shelves generate less MPCs. Therefore, a larger Rician  $K$  factor is observed in the intelligent forklift truck scenario.

**Table 4.** Parameters of fitted CDFs for Rician  $K$  factor.

Scenarios	Parameters	
	$\mu_{\log\text{-normal}}$	$\sigma_{\log\text{-normal}}$
Intelligent forklift truck	4.16	0.93
Stacking and shuttle car	0.70	1.46
AGV (LOS)	1.71	1.86

**Figure 11.** Empirical and fitted CDFs of Rician  $K$  factor.

#### 4. Conclusions

In this paper, a mmWave channel measurement campaign at 28 GHz was conducted in smart warehouse scenarios. The smart warehouse includes three different sub-scenarios, which are an intelligent forklift truck scenario, a stacking and shuttle car scenario, and an AGVs scenario. A VNA-based channel sounder was used to perform measurements in different sub-scenarios. Based on mmWave channel measurements, key large-scale channel parameters were calculated and the statistical properties were extracted and analyzed. In the stacking and shuttle car scenario, because Rx is located inside the stack, there are some obstructions to the LOS path between transceivers. Therefore, the path loss of this scenario is the largest among all sub-scenarios. Meanwhile, the obstruction of metal sheets for MPCs in the stack resulted in the smallest delay spread and Rician  $K$  factor among all sub-scenarios. In addition, the AGV scenario and the intelligent forklift truck scenario exhibit the largest RMS delay spread and Rician  $K$  factor, respectively. From the analysis results of large-scale channel parameters, it is found that there are still relatively rich MPCs in smart warehouse scenarios. This is due to the presence of scatterers near the transceiver. Although part of the MPCs is obstructed by metal sheets in the sub-scenarios of stacking and shuttle car, there are still enough MPCs to provide channel capacity for communication. This situation is consistent with most references that conducted mmWave channel measurements in industrial scenarios. However, the more significant mobility of robots in smart warehouses leads to a higher probability of the OLOS condition compared to industrial scenarios. For example, the AGVs carrying freight containers can frequently obstruct each other in the AGVs scenario, resulting in dynamic changes of the LOS and OLOS conditions. Due to the higher penetration loss based on the analysis results, the OLOS condition has a significant, negative impact on mmWave communication system performance. Therefore, accurate path planning and trajectory control are necessary to reduce the probability of OLOS conditions, especially in some high-mobility smart warehouse scenarios. In addition, the large-scale channel parameters and statistical properties provided in this paper can be used in the link evaluation and system design of communication networks in smart warehouses.

**Author Contributions:** Conceptualization, H.M. and B.A.; methodology, R.H.; software, H.M.; validation, H.M.; formal analysis, H.M.; investigation, X.Z.; resources, X.Z.; data curation, H.M. and X.Z.; writing—original draft preparation, H.M.; writing—review and editing, R.H.; visualization, H.Z.; supervision, B.A. and Z.Z.; project administration, R.C. and T.W.; funding acquisition, B.A. and X.Z. All authors have read and agreed to the published version of the manuscript.

**Funding:** This research was funded by the National Key R&D Program of China under Grant 2022YFF0608103, 2022YFF0604805, 2021YFB2900301, 2020YFB1806604 and 2021YFB3901302, National Natural Science Foundation of China under Grant 62221001, Fundamental Research Funds for the Central Universities 2022JBQY004, Natural Science Foundation of Jiangsu Province Major Project under Grant BK20212002, Young Elite Scientists Sponsorship Program by CAST under Grant 2022QNRC001 and the Science and technology project of China Academy of Railway Sciences 2022YJ033.

**Data Availability Statement:** The data presented in this study are available on request from the corresponding author. The data are not publicly available due to privacy restrictions.

**Acknowledgments:** The authors would like to thank Chengyi Zhou and Huichao Shang from Beijing Jiaotong University for their help with the wireless channel measurements.

**Conflicts of Interest:** The authors declare no conflict of interest.

## References

1. Zhen, L.; Li, H. A literature review of smart warehouse operations management. *Front. Eng. Manag.* **2022**, *9*, 31–55. [\[CrossRef\]](#)
2. Kamali, A. Smart warehouse vs. traditional warehouse. *CiiT. Int. J. Autom. Auton. Syst.* **2019**, *11*, 9–16.
3. Lee, Y.; Kim, J.; Lee, H.; Moon, K. IoT-based data transmitting system using a UWB and RFID system in smart warehouse. In Proceedings of the 2017 Ninth International Conference on Ubiquitous and Future Networks (ICUFN), Milan, Italy, 4–7 July 2017; pp. 545–547. [\[CrossRef\]](#)
4. Cogo, E.; Žunić, E.; Beširević, A.; Delalić, S.; Hodžić, K. Position based visualization of real world warehouse data in a smart warehouse management system. In Proceedings of the 2020 19th International Symposium INFOTEH-JAHORINA (INFOTEH), East Sarajevo, Bosnia and Herzegovina, 18–20 March 2020; pp. 1–6. [\[CrossRef\]](#)
5. Liu, X.; Cao, J.; Yang, Y.; Jiang, S. CPS-based smart warehouse for industry 4.0: A survey of the underlying technologies. *Computers* **2018**, *7*, 13. [\[CrossRef\]](#)
6. Žunić, E.; Delalić, S.; Hodžić, K.; Beširević, A.; Hindija, H. Smart warehouse management system concept with implementation. In Proceedings of the 2018 14th Symposium on Neural Networks and Applications (NEUREL), Belgrade, Serbia, 20–21 November 2018; pp. 1–5.
7. Sung, W.T.; Lu, C.Y. Smart warehouse management based on IoT architecture. In Proceedings of the 2018 International Symposium on Computer, Consumer and Control (IS3C), Taichung, Taiwan, 6–8 December 2018; pp. 169–172.
8. Tang, Y.M.; Ho, G.T.S.; Lau, Y.Y.; Tsui, S.Y. Integrated smart warehouse and manufacturing management with demand forecasting in small-scale cyclical industries. *Machines* **2022**, *10*, 472. [\[CrossRef\]](#)
9. He, R.; Ai, B.; Zhong, Z.; Yang, M.; Chen, R.; Ding, J.; Ma, Z.; Sun, G.; Liu, C. 5G for Railways: Next Generation Railway Dedicated Communications. *IEEE Commun. Mag.* **2022**, *60*, 130–136. [\[CrossRef\]](#)
10. Khurpade, J.M.; Rao, D.; Sanghavi, P.D. A Survey on IOT and 5G Network. In Proceedings of the 2018 International Conference on Smart City and Emerging Technology (ICSCET), Mumbai, India, 5 January 2018; pp. 1–3. [\[CrossRef\]](#)
11. Song, Y.; Yu, F.R.; Zhou, L.; Yang, X.; He, Z. Applications of the Internet of Things (IoT) in Smart Logistics: A Comprehensive Survey. *IEEE Internet Things J.* **2021**, *8*, 4250–4274. [\[CrossRef\]](#)
12. Das, A.K.; Roy, S.; Bandara, E.; Shetty, S. Securing Age-of-Information (AoI)-Enabled 5G Smart Warehouse Using Access Control Scheme. *IEEE Internet Things J.* **2023**, *10*, 1358–1375. [\[CrossRef\]](#)
13. Nath, S.; Sarkar, B. An integrated cloud manufacturing model for warehouse selection in a smart supply chain network: A comparative study. *J. Inst. Eng. Ser. C* **2020**, *101*, 25–41. [\[CrossRef\]](#)
14. Al-Shammari, B.K.J.; Hburi, I.; Idan, H.R.; Khazaa, H.F. An Overview of mmWave Communications for 5G. In Proceedings of the 2021 International Conference on Communication & Information Technology (ICICT), Basrah, Iraq, 5–6 June 2021; pp. 133–139. [\[CrossRef\]](#)
15. He, R.; Ai, B.; Stüber, G.L.; Wang, G.; Zhong, Z. Geometrical-Based Modeling for Millimeter-Wave MIMO Mobile-to-Mobile Channels. *IEEE Trans. Veh. Technol.* **2018**, *67*, 2848–2863. [\[CrossRef\]](#)
16. Ma, Z.; Ai, B.; He, R.; Zhong, Z.; Yang, M. A Non-Stationary Geometry-Based MIMO Channel Model for Millimeter-Wave UAV Networks. *IEEE J. Sel. Areas Commun.* **2021**, *39*, 2960–2974. [\[CrossRef\]](#)
17. He, R.; Schneider, C.; Ai, B.; Wang, G.; Zhong, Z.; Dupleich, D.A.; Thomae, R.S.; Boban, M.; Luo, J.; Zhang, Y. Propagation Channels of 5G Millimeter-Wave Vehicle-to-Vehicle Communications: Recent Advances and Future Challenges. *IEEE Veh. Technol. Mag.* **2020**, *15*, 16–26. [\[CrossRef\]](#)
18. Busari, S.A.; Huq, K.M.S.; Mumtaz, S.; Dai, L.; Rodriguez, J. Millimeter-Wave Massive MIMO Communication for Future Wireless Systems: A Survey. *IEEE Commun. Surv. Tutor.* **2018**, *20*, 836–869. [\[CrossRef\]](#)

19. Uwaechia, A.N.; Mahyuddin, N.M. A Comprehensive Survey on Millimeter Wave Communications for Fifth-Generation Wireless Networks: Feasibility and Challenges. *IEEE Access* **2020**, *8*, 62367–62414. [[CrossRef](#)]
20. Alsabah, M.; Naser, M.A.; Mahmmod, B.M.; Abdhulhussain, S.H.; Eissa, M.R.; Al-Baidhani, A.; Noordin, N.K.; Sait, S.M.; Al-Utaibi, K.A.; Hashim, F. 6G Wireless Communications Networks: A Comprehensive Survey. *IEEE Access* **2021**, *9*, 148191–148243. [[CrossRef](#)]
21. He, R.; Ai, B.; Wang, G.; Yang, M.; Huang, C.; Zhong, Z. Wireless Channel Sparsity: Measurement, Analysis, and Exploitation in Estimation. *IEEE Wirel. Commun.* **2021**, *28*, 113–119. [[CrossRef](#)]
22. Jiang, T.; Zhang, J.; Tang, P.; Tian, L.; Zheng, Y.; Dou, J.; Asplund, H.; Raschkowski, L.; D’Errico, R.; Jämsä, T. 3GPP Standardized 5G Channel Model for IIoT Scenarios: A Survey. *IEEE Internet Things J.* **2021**, *8*, 8799–8815. [[CrossRef](#)]
23. Gulia, R.S.; Mamun, S.A.; Vashist, A.; Ganguly, A.; Hochgraf, C.; Kwasinski, A.; Kuhl, M.E. Evaluation of Wireless Connectivity in an Automated Warehouse at 60 GHz. In Proceedings of the 2022 IEEE International Conference on Consumer Electronics (ICCE), Las Vegas, NV, USA, 7–9 January 2022; pp. 1–6. [[CrossRef](#)]
24. Sun, S.; Rappaport, T.S.; Shafi, M.; Tang, P.; Zhang, J.; Smith, P.J. Propagation Models and Performance Evaluation for 5G Millimeter-Wave Bands. *IEEE Trans. Veh. Technol.* **2018**, *67*, 8422–8439. [[CrossRef](#)]
25. Wang, C.; Bian, J.; Sun, J.; Zhang, W.; Zhang, M. A Survey of 5G Channel Measurements and Models. *IEEE Commun. Surv. Tutor.* **2018**, *20*, 3142–3168. [[CrossRef](#)]
26. Pang, L.; Zhang, J.; Zhang, Y.; Huang, X.; Chen, Y.; Li, J. Investigation and comparison of 5G channel models: From QuaDRiGa, NYUSIM, and MG5G perspectives. *Chin. J. Electron.* **2022**, *31*, 1–17.
27. Mi, H.; Ai, B.; He, R.; Zhou, X.; Ma, Z.; Yang, M.; Zhong, Z. Millimeter Wave Channel Measurement and Analysis in Smart Warehouse Scenario. In Proceedings of the 2022 IEEE International Symposium on Antennas and Propagation and USNC-URSI Radio Science Meeting (AP-S/URSI), Denver, CO, USA, 10–15 July 2022; pp. 211–212. [[CrossRef](#)]
28. Cano, C.; Sim, G.H.; Asadi, A.; Vilajosana, X. A Channel Measurement Campaign for mmWave Communication in Industrial Settings. *IEEE Trans. Wirel. Commun.* **2021**, *20*, 299–315. [[CrossRef](#)]
29. Osa, J.; Björnell, N.; Ångskog, P.; Val, I.; Mendicuti, M. 60 GHz mmWave Signal Propagation Characterization in Workshop and Steel Industry. In Proceedings of the 2023 IEEE 19th International Conference on Factory Communication Systems (WFCS), Pavia, Italy, 26–28 April 2023; pp. 1–8. [[CrossRef](#)]
30. Wang, Y.; Jiang, T.; Tang, P.; Song, Q.; Zhao, X.; Tian, L.; Zhang, J.; Liu, B. Measurement-based Analysis and Modeling of Channel Characteristics in an Industrial Scenario at 28 GHz. In Proceedings of the 2021 IEEE 94th Vehicular Technology Conference (VTC2021-Fall), Virtual, 27 September–28 October 2021; pp. 1–5. [[CrossRef](#)]
31. Schmieder, M.; Undi, F.; Peter, M.; Koenig, E.; Keusgen, W. Directional Wideband Channel Measurements at 28 GHz in an Industrial Environment. In Proceedings of the 2019 IEEE Global Communications Conference (GLOBECOM), Big Island, HI, USA, 9–13 December 2019; pp. 1–6. [[CrossRef](#)]
32. Schmieder, M.; Eichler, T.; Wittig, S.; Peter, M.; Keusgen, W. Measurement and Characterization of an Indoor Industrial Environment at 3.7 and 28 GHz. In Proceedings of the 2020 14th European Conference on Antennas and Propagation (EuCAP), Copenhagen, Denmark, 15–20 March 2020; pp. 1–5. [[CrossRef](#)]
33. Fleury, B.; Tschudin, M.; Heddergott, R.; Dahlhaus, D.; Ingeman Pedersen, K. Channel parameter estimation in mobile radio environments using the SAGE algorithm. *IEEE J. Sel. Areas Commun.* **1999**, *17*, 434–450. [[CrossRef](#)]
34. Mi, H.; Ai, B.; He, R.; Zhou, X.; Ma, Z.; Yang, M.; Zhong, Z.; Wang, N. Multi-scenario millimeter wave wireless channel measurements and sparsity analysis. *China Commun.* **2022**, *19*, 16–31. [[CrossRef](#)]
35. Ai, B.; Guan, K.; He, R.; Li, J.; Li, G.; He, D.; Zhong, Z.; Huq, K.M.S. On Indoor Millimeter Wave Massive MIMO Channels: Measurement and Simulation. *IEEE J. Sel. Areas Commun.* **2017**, *35*, 1678–1690. [[CrossRef](#)]
36. Document TR38.901 V16.1.0, 3GPP. Study on Channel Model for Frequencies from 0.5 to 100 GHz. 2020. Available online: <https://portal.3gpp.org/desktopmodules/Specifications/SpecificationDetails.aspx?specificationId=3173> (accessed on 11 January 2020).
37. Kyosti, P. WINNER II Channel Models. Ist Technical Report Ist-4-027756 Win. Ii D1. 1.2 V1. 2. 2007. Available online: <https://www.mathworks.com/help/comm/ug/winner-ii-channel.html> (accessed on 30 September 2007).
38. Sun, S.; Rappaport, T.S.; Thomas, T.A.; Ghosh, A.; Nguyen, H.C.; Kovács, I.Z.; Rodriguez, I.; Koymen, O.; Partyka, A. Investigation of Prediction Accuracy, Sensitivity, and Parameter Stability of Large-Scale Propagation Path Loss Models for 5G Wireless Communications. *IEEE Trans. Veh. Technol.* **2016**, *65*, 2843–2860. [[CrossRef](#)]
39. Cai, X.; Zhang, G.; Zhang, C.; Fan, W.; Li, J.; Pedersen, G.F. Dynamic Channel Modeling for Indoor Millimeter-Wave Propagation Channels Based on Measurements. *IEEE Trans. Commun.* **2020**, *68*, 5878–5891. [[CrossRef](#)]
40. Friis, H.T. A note on a simple transmission formula. *Proc. IRE* **1946**, *34*, 254–256. [[CrossRef](#)]
41. Erden, F.; Ozdemir, O.; Guvenc, I. 28 GHz mmWave Channel Measurements and Modeling in a Library Environment. In Proceedings of the 2020 IEEE Radio and Wireless Symposium (RWS), San Antonio, TX, USA, 26–29 January 2020; pp. 52–55. [[CrossRef](#)]
42. Liu, Y.; Guo, X.; Lin, L. Wideband Channel Measurement Over the Horizon. In Proceedings of the 2018 12th International Symposium on Antennas, Propagation and EM Theory (ISAPE), Hangzhou, China, 3–6 December 2018; pp. 1–2. [[CrossRef](#)]

43. Wang, L.; Ai, B.; He, D.; Yi, H.; Zhong, Z.; Kim, J. Channel characterisation in rural railway environment at 28 GHz. *IET Microw. Antennas Propag.* **2019**, *13*, 1052–1059. [[CrossRef](#)]
44. Chen, Y.; Beaulieu, N. Maximum likelihood estimation of the K factor in Ricean fading channels. *IEEE Commun. Lett.* **2005**, *9*, 1040–1042. [[CrossRef](#)]

**Disclaimer/Publisher's Note:** The statements, opinions and data contained in all publications are solely those of the individual author(s) and contributor(s) and not of MDPI and/or the editor(s). MDPI and/or the editor(s) disclaim responsibility for any injury to people or property resulting from any ideas, methods, instructions or products referred to in the content.